Journal of Hydrology 468–469 (2012) 130–138

Contents lists available at SciVerse ScienceDirect

Journal of Hydrology

journal homepage: www.elsevier.com/locate/jhydrol

A multi-model approach for improved simulations of future water availability at a large Eastern Mediterranean karst spring

Andreas Hartmann [a,*], Jens Lange [a], Àngela Vivó Aguado [a], Numan Mizyed [b], Gerhard Smiatek [c], Harald Kunstmann [c]

[a] Institute of Hydrology, Freiburg University, Fahnenbergplatz, 79098 Freiburg, Germany
[b] Civil Engineering Department, An-Najah National University, Nablus, Palestine
[c] Institute for Meteorology and Climate Research (IMK-IFU), Karlsruhe Institute of Technology (KIT), Kreuzeckbahnstr. 19, 82467 Garmisch-Partenkirchen, Germany

ARTICLE INFO

Article history:
Received 18 June 2012
Received in revised form 7 August 2012
Accepted 15 August 2012
Available online 27 August 2012
This manuscript was handled by Peter K. Kitanidis, Editor-in-Chief, with the assistance of Barbara J. Mahler, Associate Editor

Keywords:
Climate change
Groundwater abstraction
Karst hydrology
Conceptual modeling
Mediterranean karst
Faria spring

SUMMARY

Recent studies identified the Mediterranean as a region particularly vulnerable to climate change. Since a large fraction of the region's water originates from karst aquifers, information about their future water availability is important for sustainable water management. This study presents an ensemble of 50 model chains considering five different realisations of the A1B ECHAM5 and HadCM3 climate projections, two different averaging methods to transfer the climate variables to the system scale and five different hydrological models that represent reasonable conceptualizations of the karst system. The ensemble is applied to Faria spring, a large Eastern Mediterranean karst spring in the West Bank. We show that for the near future (2021–2051) variability resulting from the different climate change projections and five different models is too large to draw conclusions on any significant change. In the remote future (2068–2098), variability decreases and our simulations suggest a decrease of water availability of −15% to −30%. We also assess the impact of recent pumping activities by running our hydrological models with recently measured data. There is a strong indication that the spring, which dried out in 2007, would have still yielded significant amounts of water if groundwater extractions had been limited. This calls for a better management of groundwater abstractions to meet future water needs in this drought-prone Mediterranean region.

1. Introduction

Climate projections indicate a significant rise of global temperatures together with decreasing precipitation in the Mediterranean region (Giorgi and Lionello, 2008). Also recent studies identified the Mediterranean area as a hot spot of aggravated droughts and heat waves in the coming decades (Orlowsky and Seneviratne, 2012). Approximately 35% of Europe's land surface are karst exposures and some of its countries receive up to 50% of their drinking water from karst systems (Andreo et al., 2006). Most karst exposures are found in the Mediterranean region. For instance 25% of Spain, 33% of France and Turkey, and more than 40% of Slovenia and Croatia are covered by carbonate rocks (Lewin and Woodward, 2009). Therefore, a profound knowledge about global change impacts on karst water resources is important for water resources management at these regions, especially at the Eastern Mediterranean, where trans-boundary water agreements are necessary to share water resources among different countries (e.g. Brooks and Trottier, 2010). However, the manner how changes will affect local or regional water budgets is difficult to assess (Seiler and Gat, 2007). One possible way is to apply hydrological models, which transform climatic into hydrological projections. For reliable simulations, the used models require an adequate representation of hydrological systems, which is particularly true in karst regions.

In general, two different types of process-based hydrological models can be distinguished for karst systems: distributed and lumped (Sauter et al., 2006). Distributed provide spatially distributed information about groundwater heads and flow, including karst processes in different degrees of complexity (for an overview see Goldscheider and Drew, 2007). Lumped models are based on a set of mathematical equations that represent the transfer from input. Karst processes can be included conceptually (e.g. Butscher and Huggenberger, 2008; Fleury et al., 2007; Hartmann et al., 2012; Rimmer and Salingar, 2006; Tritz et al., 2011). In most cases, the complexity and heterogeneity of karst systems and the lack or limitation of groundwater monitoring data prohibit the use of distributed models and lumped models are applied (Jukic and Denic-Jukic, 2009).

There are many studies that coupled climate models with hydrological models (Lenderink et al., 2007; Stoll et al., 2010),

* Corresponding author. Tel./fax: +49 761 203 97832.
E-mail address: andreas.hartmann@hydrology.uni-freiburg.de (A. Hartmann).

0022-1694/$ - see front matter © 2012 Elsevier B.V. All rights reserved.
http://dx.doi.org/10.1016/j.jhydrol.2012.08.024

but only a few of them were performed in karst areas: using a distributed model, Loaiciga et al. (2000) investigated the impact of climate change on the Edwards Balcones Fault Zone karst aquifer Texas, USA. They found a future threatening of water availability if present pumping rates will not be adapted to future changes in recharge conditions. Applying a conceptual approach to a large karst spring in China, Hao et al. (2006) showed a decrease of spring discharge, which could primarily be attributed to climate change. Using a groundwater model (Brouyère et al., 2003) predicted a decrease of groundwater levels in relation to variations in climatic conditions in a chalky aquifer in Belgium. In the Eastern Mediterranean, Samuels et al. (2010) coupled a conceptual karst model with a regional climate model. They found that the predicted decrease of precipitation in the middle of this century will result in reduced stream flow, aggravated by increased evaporation. Similar results for the same area were found by Smiatek et al. (2011).

This study addresses the impact of global climate change on Faria Spring, a major Mediterranean karst spring, located 10 km northeast of the city of Nablus, West Bank, Palestinian Authority. In order to account for variability in climate change simulations, in extracting and averaging their gridded information, and in the choice of an adequate hydrological model, we built an ensemble of 50 different data sets. Data from five dynamic downscaling experiments with A1B scenario boundary forcings from the ECHAM5 and HadCM3 climate models were bias-corrected and related to the spring area in two different ways. Results were used as input for five lumped process-based hydrological karst models that were previously calibrated by historic discharge observations. After plausibility checks during a control period (1971–2001), we produced ensemble runs for two future periods (2021–2051 and 2068–2098). Finally, we compared impacts of climate change to recent changes in spring discharge following increased groundwater abstractions.

2. Study area

The Faria catchment, extending for about 30 km from west to east, lies within the Eastern Mountain Aquifer Basin, which is one of the three major groundwater aquifer basins forming the West Bank groundwater resources (EXACT, 1998). The Faria spring is located about 10 km northeast of the city of Nablus at an elevation of 160 m a.s.l. (Fig. 1). Until recently, it has been one of the largest fresh water springs in the West Bank (PWA, 2000).

The West Bank has a semi-arid, Mediterranean climate. The rainy season lasts from October to April with 90% of the rainfall occurring in autumn and winter. Summer months are characterized by high potential evaporation and only occasional rain events may occur. In the Faria catchment, mean annual precipitation ranges from 640 mm in the headwaters down to 150 mm at the outlet to the Jordan River. The mean annual temperature varies from 18 °C in the western headwaters to 24 °C in the eastern lower parts (Shadeed and Lange, 2010).

Faria spring discharges approximately 30 km^2 of karstified Eocene calcareous rock (Fig. 1c). From 1963 to 1999 the average annual discharge was 5.3×10^6 m^3. In 1978/1979, the driest year during this period, the discharge dropped down to of 16 l s^{-1} in August. Then water from spring was not sufficient to irrigate the 50 ha of agricultural land around the spring. But the spring never dried out completely. Historically, the spring was an important fresh water resource for both domestic and agricultural use in the West Bank. Due to the availability of agricultural land in the western surroundings of the spring, Jordanian authorities gave permission to drill eight irrigation wells in the early 1960s. After 1967, further drilling was restricted and the amount of pumping from the aquifer continued to be nearly constant, ranging from 1.5 to 2.0×10^6 m^3 per year (PWA, 2000). Pumping from existing wells increased after 1995. In addition, uncontrolled and unorganized drilling activities started. Until 2007 more than 30 wells had been drilled in the area producing approximately 10×10^6 m^3 of irrigation water per year. At least one of these wells reached the base of the Eocene aquifer. As a result, the spring started drying out and it is presently completely dry (Fig. 2).

3. Materials and methods

3.1. Hydrological models

3.1.1. Model structures

We chose five different lumped models to account for uncertainties in the choice of hydrological model structures (Fig. 3). Uncertainty in model parameters may also limit the validity of land-use or climate change predictions (Wagener et al., 2001). Thus, we only used models with three to six parameters, which is the maximum number that can be identified from a single time series of discharge (Beven, 1989; Jakeman and Hornberger, 1993).

All models consider karst hydrological processes in different ways and complexity. They consist of an overflow routine that constitutes the soil/epikarst, and different combinations of linear reservoirs that represent the vadose and the groundwater zones. The overflow routine is characterized by a water volume $V_{OS}(t)$ that varies according to precipitation input $P(t)$, and according to actual evapotranspiration $E_{act}(t)$ and groundwater recharge $R(t)$ as outputs. Similar to many other models (e.g. HBV, Bergström, 1995; TOPMODEL, Beven and Kirby, 1979), $E_{act}(t)$ is derived from:

$$E_{act}(t) = E_{pot}(t) \cdot \frac{V_{OS}(t)}{V_{OS,\max}} \quad (1)$$

where $E_{pot}(t)$ is the potential evaporation derived by the Hargreaves method (Hargreaves and Samani, 1985) and $V_{OS,\max}$ a parameter describing the maximum holding capacity of the soil and the epikarst. When $V_{OS}(t)$ exceeds $V_{OS,\max}$, the excess water recharges the groundwater routine below:

$$R(t) = \max(V_{OS}(t) - V_{OS,\max}, 0) \cdot A \quad (2)$$

where A is the recharge area to the spring. The applied groundwater routines have already been used in different karst modeling studies. The simple model (Fig. 3a) consists of a single linear reservoir as originally been used by Maillet (1905). The serial model (Fig. 3b) consists of two linear reservoirs in series, the upper one representing the vadose zone and the lower one representing the groundwater system (e.g. Rimmer and Salingar, 2006). The parallel model (Fig. 3d) is made of two parallel linear reservoirs representing a conduit and a matrix groundwater system (e.g. Fleury et al., 2007). The combined model (Fig. 3c) is similar to the parallel model, but water from the matrix has to pass the conduit system before it reaches the spring (e.g. in Geyer et al., 2007). The exchange model (Fig. 3e) is again similar to the parallel model, but allows for water exchange between matrix and conduits depending of the water levels and porosities of the two groundwater systems (see Rimmer and Hartmann (2012) for more details). A summary of all parameters is given in Table 1.

3.1.2. Calibration and validation

Daily rainfall and temperature data, as well as monthly measurements of spring discharge were available from 1975 to 1999. Within this period, no significant disturbances of the hydrological system by human impacts occurred. Using a daily time step, all models were individually calibrated using the Shuffled Complex Evolution algorithm (Duan et al., 1992) in a predefined, physically plausible calibration range considering preceding studies (Fleury

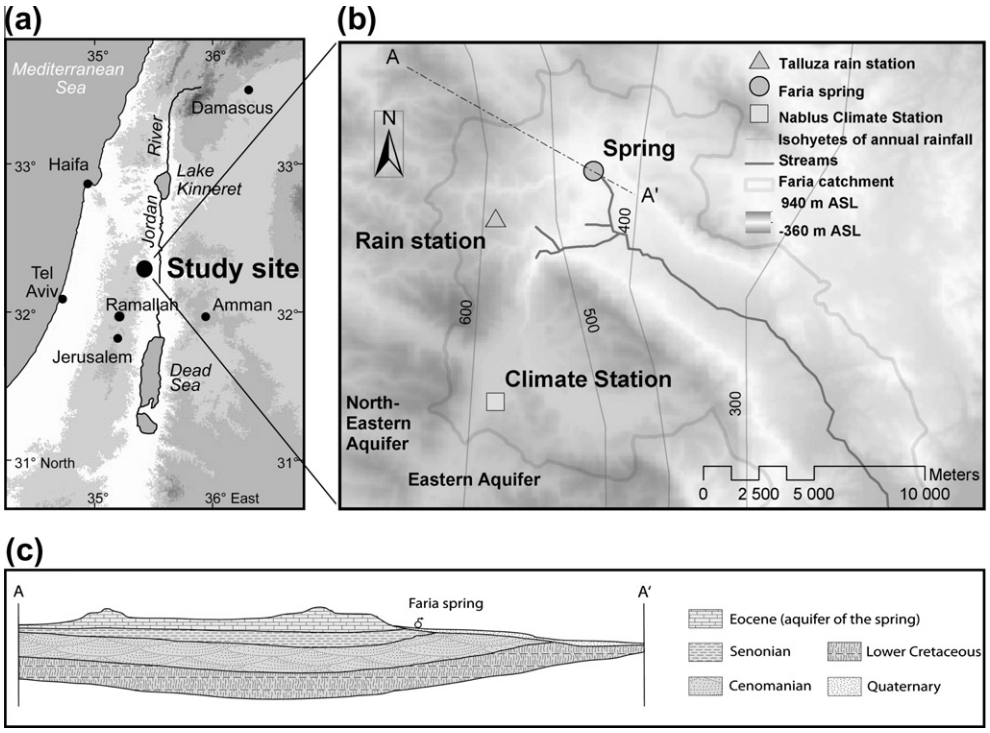

Fig. 1. (a) Location, (b) detailed map of the study area and (c) schematic cross section indicated in (b).

Fig. 2. Pictures of the spring before (April 2000) and after (March 2011) the increased pumping started.

et al., 2007; Hartmann et al., 2012; Rimmer and Salingar, 2006). To check their predictive power, we performed a split-sample test (Klemeš, 1986), i.e. we calibrated the models from 1980 to 1989 and validated their performance from 1989 to 1999. The years from 1975 to 1979 were used as a warm up to account for uncertainties in initial conditions. For calibration as well as for validation the Nash Sutcliffe efficiency NSE (Nash and Sutcliffe, 1970) served as objective function.

3.2. Regional climate change projections

Climate change data were derived from transient dynamical downscaling experiments with Regional Climate Models (RCMs). The employed RCMs were RegCM3 (Pal et al., 2000) and two versions of the NCAR/Penn State University MM5 model (Dudhia, 1993). The MM5 models mainly differ in the employed soil vegetation atmosphere transfer scheme (SVAT). The RCMs were driven with boundary forcings from two versions of the ECHAM5 (realizations 1 and 3) and the HadCM3 general circulation models (GCMs) using the A1B emission scenario. Table 2 shows a list of the applied models, their main configurations and provides sources for further information. Krichak et al. (2011), Smiatek et al. (2011) and Samuels et al. (2011) evaluated the different RCMs in the Eastern Mediterranean region. RCMs were able to reproduce observed precipitation patterns, but had shortcomings in precipitation seasonality. In contrast to observations, they showed a monthly precipitation peak in December instead of January. Therefore, a bias-correction was necessary.

Daily simulated precipitation data were corrected using the quantile to quantile approach (Déqué et al., 2007). Two gridded and one local data set were available to assess quantiles of the observed precipitation: (1) regionalized, gridded, 1×1 km^2 precipitation data used in the Jordan River region (JR, Menzel et al., 2009), (2) gridded European precipitation data at 0.25° resolution (E-OBS, Version 5.0; Haylock et al., 2008; van den Besselaar et al., 2011), and (3) a local time series of precipitation collected at Talluza station (Fig. 1). Fig. 4a shows the mean monthly precipitation for the three data sources in the area of Talluza. It can be seen, that

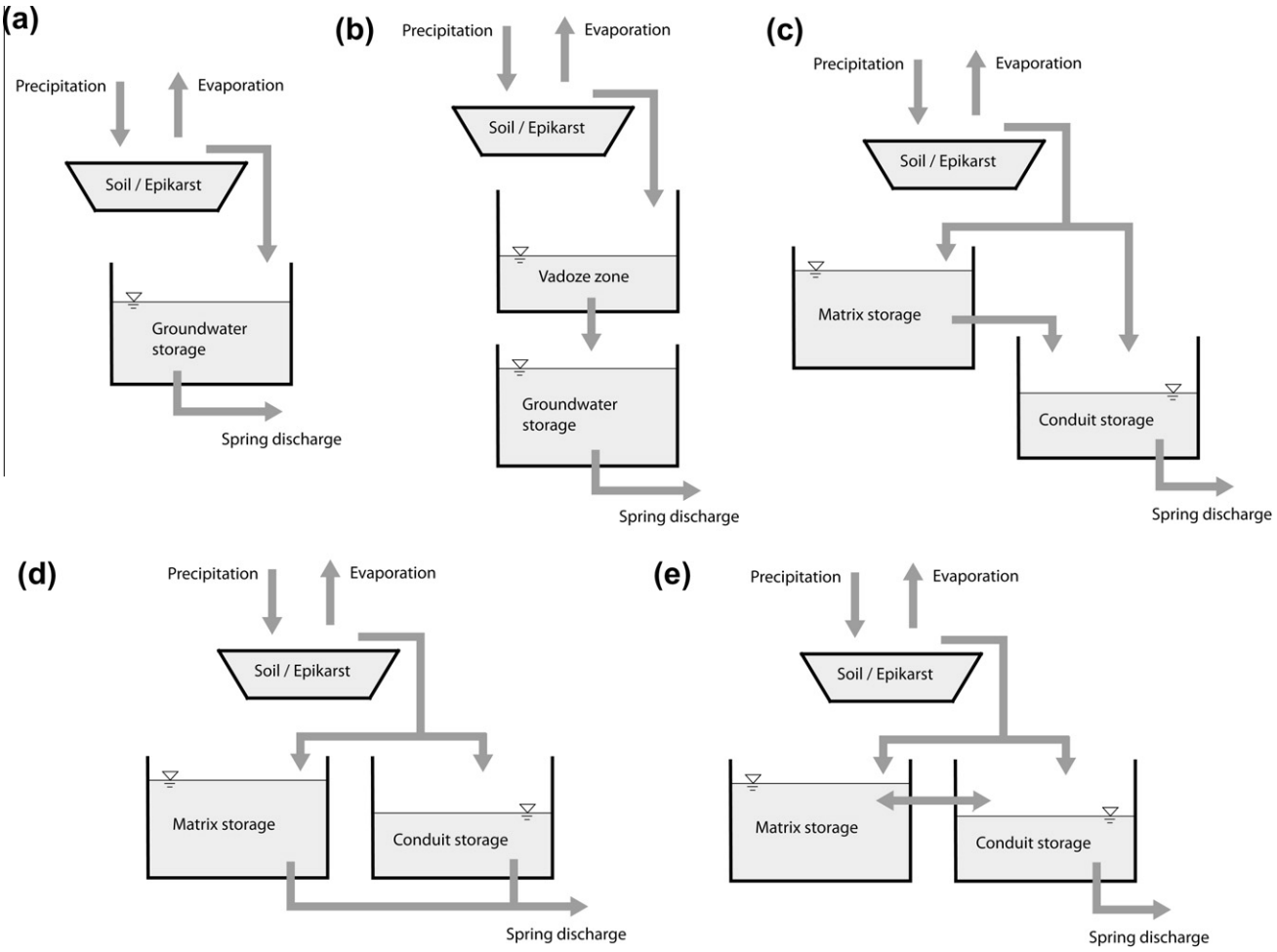

Fig. 3. The hydrological model ensemble: (a) simple model, (b) serial model, (c) combined model, (d) parallel model, and (e) exchange model.

Table 1
Model parameters, description, calibrated parameter values, NSEs during the calibration/validation periods and calibration ranges (empty fields indicate that this parameter is not included in the model).

Parameter	Description	Unit	Model					Ranges	
			Simple	Parallel	Series	Kombi	Exchange	Lower	Upper
$V_{OS,max}$	Soil/Epikarst storage capacity	mm	166	166	126	126	126	0	500
A	Recharge area	km^2	33.3	33.3	27.2	27.1	27.1	20	50
K	Groundwater storage constant	d	665		505			0	1000
K_{VZ}	Vadose zone storage constant	d			36			0	100
f	Recharge separation factor	–		7.70E−09		0.04	0.06	0	1
K_1	Fast groundwater storage constant	d		61		64	81	0	100
K_2	Slow groundwater storage constant	d		665		486		100	1000
K_E	Groundwater exchange constant	d					370	100	1000
f_P	Porosity difference factor	–					1	1	100
NS_{cal}	Nash Sutcliffe efficiency calibration	–	0.76	0.76	0.81	0.82	0.82	–	–
NS_{val}	Nash Sutcliffe efficiency validation	–	0.78	0.78	0.77	0.78	0.77	–	–

both JR and the E-OBS data, substantially underestimate rainfall over the entire rainy season. Thus, Talluza station data was used for the bias-correction.

The hydrological models additionally require temperature data to calculate potential evapotranspiration. Most climate projections tended to overestimate observed temperature at Nablus meteorological station (Fig. 1b) from summer to winter. In spring, the opposite was observed. The projection mean, however, only showed marginal deviation from observed data. Hence, we decided to refrain from bias correction for temperature.

3.3. Coupling of climate models and hydrological models

The five realizations of the climate models provided gridded time series of precipitation and temperature (Table 2). For transferring the gridded information to the karst system scale, we averaged (1) the four grid points surrounding the estimated recharge area and (2) the two grid points at the Eastern side of the estimated recharge area, that were expected to differ most from the four point average because they receive less precipitation due to the regional rainfall gradient (Fig. 1b). Overall, we coupled five realizations of

Table 2
Applied climate change simulation data (number in bracket refers to realization).

Acronym	Driving GCM (realization)	RCM	SVAT	Grid size (km)	Institution reference
V35E	ECHAM5(1)	MM5 V3.5	OSU LSM	18.6	KIT/IMK-IFU (Smiatek et al., 2011)
V35H	HadCM3(1)	MM5 V3.5	OSU LSM	18.6	
V37E	ECHAM5(1)	MM5 V3.7	Noah LSM	18.6	
V37H	HadCM3(1)	MM5 V3.7	Noah LSM	18.6	
RCM3	ECHAM5(3)	RegCM3	BATS	25	TAU (Krichak et al., 2011)

climates projections, two different ways of averaging their output and five different hydrological models. During a control time period (1971–2001) we compared the mean discharge of our 50 member ensemble with the simulations of the hydrological models that used measured precipitation and temperature as input. For future runs, we considered two 30-year time periods: (1) the near future 2021–2051 and (2) the remote future 2068–2098. Since the RegCM3 climate projections (Table 2) ended in 2061, simulation runs for the remote future period could only be performed with the MM5 projections that ran until 2098.

3.4. Impact of pumping

Similar to the approach presented by Hao et al. (2009), we assessed the effect of increased pumping activities by applying our five hydrological models to recent data measured in a period after model validation (1999–2010). Since the models were calibrated under natural flow conditions, they show the natural hydrological behavior of the spring. Plotting their simulations against the recent observations, they highlighted the impact of pumping. To directly compare the effects of climate change with those of pumping, we applied a delta approach. We reduced the observed time series of precipitation from 1999 to 2010 by the maximum 30-year-average precipitation decrease found in the climate simulations and ran our hydrological model ensemble again.

4. Results

4.1. Calibration and validation of the hydrological models

All models needed the entire warm-up period to approach the measurements (Fig. 5). There was no model that performed significantly better or worse than the others, both during calibration and validation (see also NSE values in Table 1). The serial model and the parallel model showed similar parameter values (Table 1). Both had larger soil/epikarst storage capacities and larger contributing areas than the other three models. In general, all models show fast and slow groundwater storage constants at similar order of magnitudes. Fast groundwater storages received only minor fractions of recharge.

4.2. Bias correction

The bias correction was able to properly adjust the mean monthly precipitation during the control period (Fig. 6a). Although the climate projection mean indicated no significant change of mean monthly precipitation in the near future (Fig. 6b), the individual realizations were highly variable: V35E and V37E showed maxima in January, E35H and E37H indicated an extremely wet February and RCM3 an extremely dry February. In the remote future (Fig. 6c), variability was smaller and a general decrease of mean monthly precipitation could be observed.

4.3. Coupling of climate models and hydrological models

During the control period, mean monthly discharges derived from the ensemble runs spread around measured discharges with high variability (Fig. 7a). Variability for actual evapotranspiration was much smaller (Fig. 7d) and its monthly values derived by the ensemble runs show only small deviations from the hydrological models driven by the historic data. Also for the near future period, ensemble discharges showed a strong heterogeneity (Fig. 7b). Three groups could be identified: (1) the HadCM3 driven E35H and E37H revealed a general increase of water availability, (2) the E35E and E37E, with boundary forcings from ECHAM5, indicated only little change, and (3) the RCM3, with the third realization of the ECHAM5 forcings, showed a strong decrease of mean monthly discharges. In the remote future period (Fig. 7c), all simulations suggested a general decrease of water availability. No significant changes occurred for actual evapotranspiration, neither in the near nor in the remote future (Fig. 7e and f).

Fig. 8 shows the relative changes of the water balance components from the control period to the two future periods. Absolute values can be found in Table 3. For the near future period, a large variability of all components, except for potential evapotranspiration, could be observed. Including their error, simulated recharge rates and discharge ranged from +40% to −45%. In the remote future period, variability decreased significantly: all climate runs indicated a decrease in available water from −15% to −30%. The spread of E_{act}, R and Q significantly increased when the hydrological models were applied.

4.4. Impact of pumping

From 2006 on, the impact of increased pumping from the aquifer became evident, since observed discharges fell below model

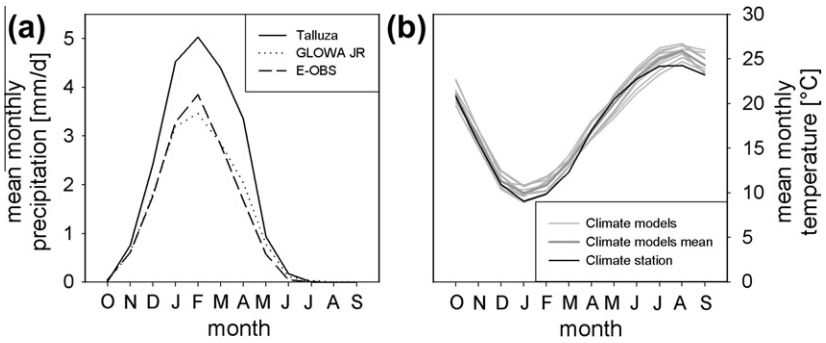

Fig. 4. Monthly mean observational references for (a) precipitation and (b) temperature (1961–1990).

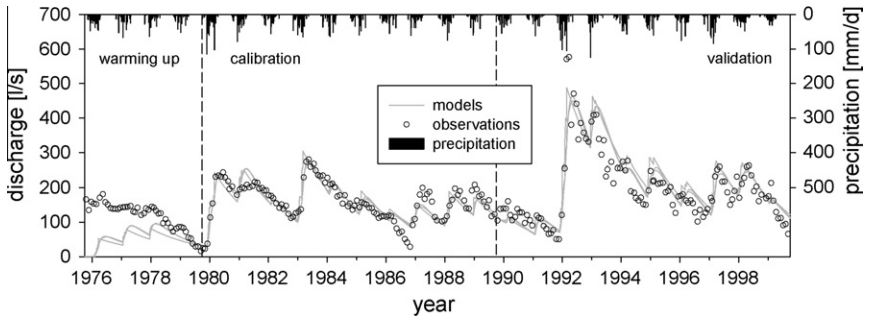

Fig. 5. Modeled and observed discharge during calibration and validation of the five hydrological models.

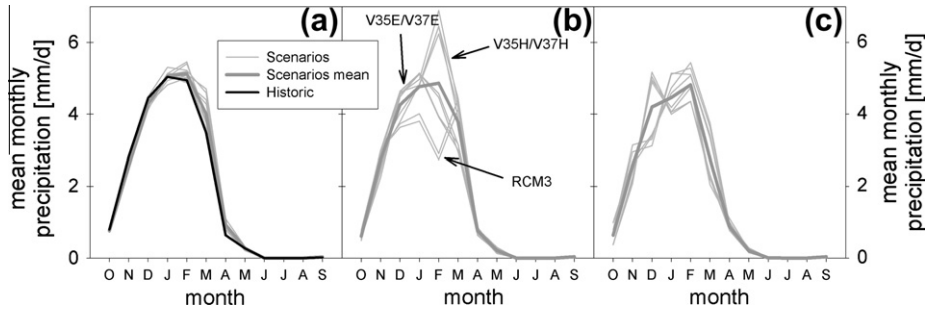

Fig. 6. Observed and climate projection mean monthly precipitation (bias corrected) for (a) the control period (1971–2001), (b) the near future period (2021–2051), and (c) the remote future period (2068–2098); note that there are no RCM3 simulations at the second future period.

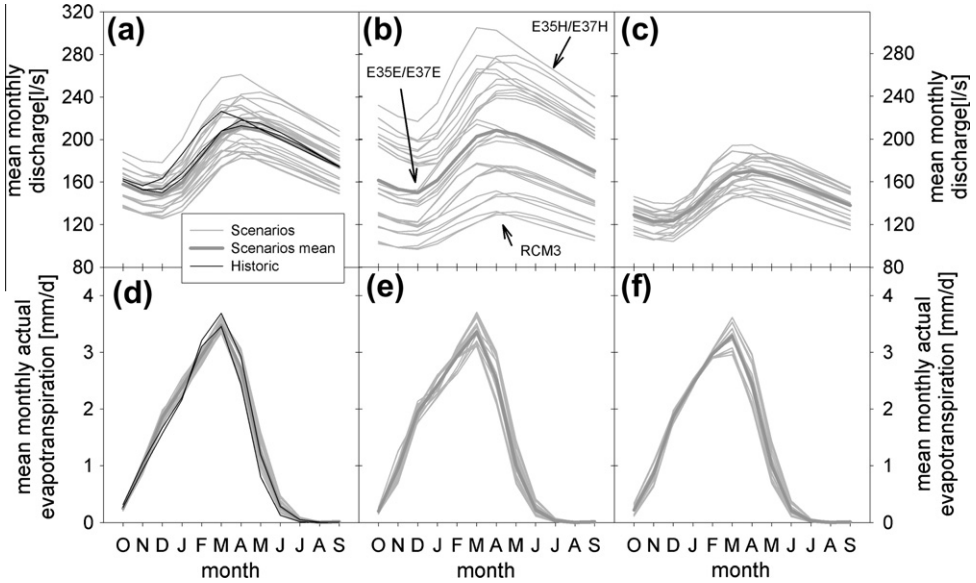

Fig. 7. Observed and climate projection mean monthly discharge and actual evapotranspiration for (a) and (d) the control period (1971–2001), (b) and (e) for the near future period (2021–2051), and (c) and (f) for the remote future period (2068–2098); note that there were no RCM3 simulations available for the remote future period.

simulations (Fig. 9). From October 2007 on the spring fell completely dry. Model simulations indicated that without pumping spring discharge would have continued.

5. Discussion

5.1. Bias correction

As in preceding studies (Alpert et al., 2008; Déqué et al., 2007), the quantile based bias correction proved reliable to account for quantitative and temporal deviations of precipitation. In the near future period, a large variability among the RCMs can be observed which is even larger than in the remote period. This was already found by Smiatek et al. (2011) and is mainly caused by single wet years with high magnitude events in spring. In our data the maximum annual rainfall amount in the near future was 1493 mm (E35H, year 2045), in the remote future period it only reached 1160 mm (E35E, year 2077). Observed differences between the MM5 and RCM3 models may have been inherited from the GCM. RCM3 employed the third; the MM5 models the first realization of ECHAM5 data. For the winter period 2021–2051, the first realization of ECHAM5 revealed a precipitation decrease of 23%, while in the third realization the simulated precipitation

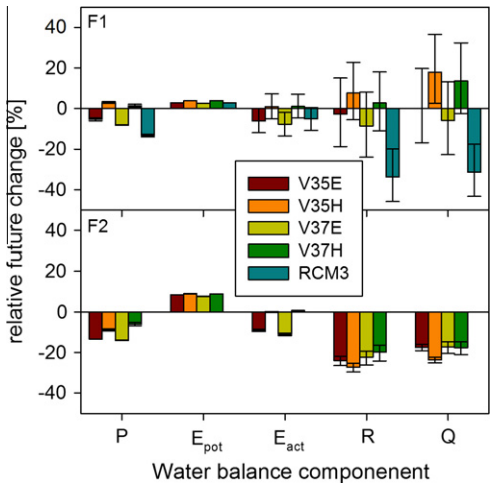

Fig. 8. Relative change in mean annual water balance components (P: precipitation, E_{pot}: potential evapotranspiration, E_{act}: actual evapotranspiration, R: recharge, Q: spring discharge) between control (1971–2001), near (F1: 2021–2051) and remote future period (F2: 2068–2098); error bars indicate maximum ranges due to differences in downscaling approaches and hydrological modeling.

decrease reached 29% in the Eastern Mediterranean. For the same period the MM5 models simulated only small precipitation changes (−1.2% to +1%) when driven with HadCM3 boundary data and minor decreases in the order of −3% when ECHAM5 was used. In RCM3, the simulated precipitation decrease was larger (−10%). These differences disappeared for the remote future period, when all RCM models simulated a precipitation decrease of up to −9%, which was similar to the results of Chenoweth et al. (2011) who found a decrease in available water resources of ∼10% for the Eastern Mediterranean and the Middle East.

5.2. Calibration of hydrological models

The temporal resolution of the discharge observations was low with approximately one measurement per month. Only the seasonal flow regime, but no fast reactions from a karstic conduit network could be characterized by this data. Hence, it was no surprise that all models containing fast and slow groundwater systems (i.e. the parallel, the combined and the exchange model) directed most of their recharge to the slow system with a small separation factor f. The storage constants for the slow systems were very high compared to other studies (Fleury et al., 2009; Geyer et al., 2008; Rimmer and Salingar, 2006) and indicated very slow system dynamics and high storage volumes that were most probably the reason why the spring never fell dry before 2000. Interestingly, the recharge area A changed among the models: the Simple and the parallel model were calibrated with larger recharge areas and with larger soil/epikarst storage capacities $V_{OS,max}$. While the structures of the other models allowed for a delay by a vadose zone (serial model) or by interaction of slow and fast system (combined and exchange model), the Simple and the parallel model produced an immediate reaction as soon as the soil/epikarst storage capacity was exceeded. Hence the necessary delay was produced by a larger $V_{OS,max}$. A "right" model could not be determined with the available data, all models had similar NSEs both for calibration and validation. Hence, it was reasonable to leave all of them in the model ensemble.

5.3. Coupling of climate models and hydrological models

The differences in the hydrological models and especially in the bias-corrected precipitation time series had a strong impact on the ensemble simulated discharges during the control period. In the near future, a high variability remained. Only the RCM3 projections predicted a significant decrease of discharge. For the second future period, all ensemble members indicate a decrease in spring discharge with much less variability. Such a decrease was also simulated in other regions in the Middle East (Heckl, 2011; Samuels et al., 2010). The water balance further showed that despite a temperature rise (expressed by higher potential evapotranspiration), the actual evapotranspiration remained almost unchanged in both future periods. Hence, the decrease in available water was mainly controlled by a decrease of precipitation. Small relative changes in annual precipitation resulted in large changes of future spring discharge.

Table 3
Water balance control (C: 1971–2001), near future period (F1: 2021–2051) and remote future period (F2: 2068–2098).

Time series	P (mm/a)			E_{pot} (mm/a)			E_{act} (mm/a)			R (mm/a)			Q (mm/a)		
	C	F1	F2	C	F1	F2	C	F1	F2	C	F1	F2	C	F1	F2
Historic	679	–	–	2275	–	–	472	–	–	207	–	–	201	–	–
V35E	692	655	599	2345	2411	2542	488	458	444	203	196	155	191	189	157
V35H	708	729	645	2231	2317	2431	478	482	478	230	246	167	213	250	163
V37E	675	620	581	2372	2433	2555	494	455	440	181	164	141	171	160	141
V37H	701	711	659	2235	2322	2432	483	487	484	218	224	175	202	229	167
RCM3	684	593	–	2336	2401	–	490	464	–	195	128	–	192	131	–

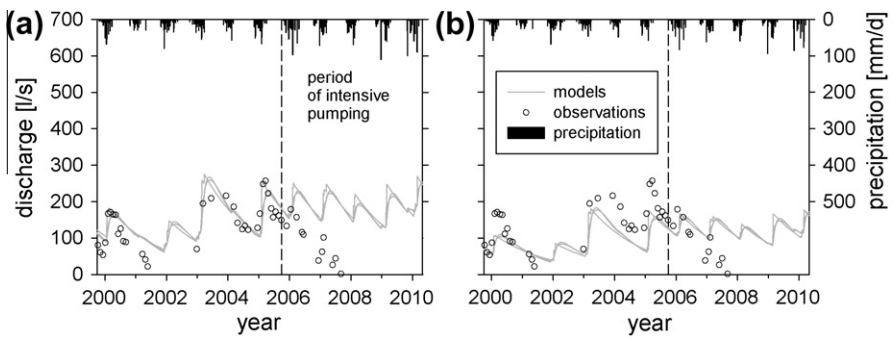

Fig. 9. Simulations of the five hydrological models from 2000 to 2010 versus the observed declining spring discharge (due to pumping).

The error for the input for each individual RCM was small (precipitation and potential evapotranspiration), indicating that the averaging by four or two grid points was not a major source of error (Fig. 8). Hydrological models again increased variability, depending on the considered time period. Differences among the RCMs were a major source of error during all periods, whereas we only found small contribution from the different ways of transferring their output to the system scale. These results partially agreed with Crosbie et al. (2011), who regarded differences between RCMs as the major source of uncertainty when coupling climate and hydrological models. However, their second largest error source was the downscaling method.

5.4. Impact of pumping

When we applied our models to more recently measured data, we found that from 2006 on the observed discharge fell below our simulations, which remained at a similar level (Fig. 9a). From October 2007 on the spring fell completely dry. Since the hydrological models only considered the natural behavior of the springs, the decrease of discharge can solely be attributed to human impacts. Thus we could show that the increased pumping activities that started 1995 (PWA, 2000) reached an unsustainable level at around 2006. In contrast to Hao et al. (2009), the impact of human activities was responsible for a 100% decrease of spring discharge, long before even one single RCM simulated a slight decrease of discharge due to climate change. When we reduced the observed precipitation by the maximum decrease of precipitation in the remote future period (V37E, decrease of precipitation of 14.4%) and ran the hydrological models ensemble with the modified data, we found a significant decrease of simulated discharges (35.3%, mean of all hydrological models), but no drying out (Fig. 9b). Hence, our study is another example of the poor groundwater management the Mediterranean region is confronted with, like e.g. in Spain (Garrido et al., 2006). Since negative effects are aggravated by climate change, prompt action is required.

6. Conclusions

In this study we investigated the future water availability of a large karst spring in a semi-arid, Eastern Mediterranean environment. The impact of climate change was determined by the coupling of hydrological models with dynamically downscaled climate change data, while the impact of increased pumping was assessed by comparing model simulations with recent observations at the spring. To address variability in the climate change simulations, we simultaneously considered five realizations of climate change simulations two different ways of transferring their gridded output to the system scale and five different hydrological models in a 50-member ensemble.

Already during a control period (1971–2001), we found large variability in simulations of the seasonal discharge behavior. The variability even increased for the near future (2021–2051), mostly due to variability in the simulated rainfall of the different RCMs. One ensemble member indicated a strong decline of discharge, while two others simulated more available water. In the remote future (2068–2098) our results were more congruent: all runs, even under the consideration of all abovementioned error sources, showed a decline in spring discharge of up to 30%. When we applied our hydrological models to recently measured data, we found that, compared to climate change, the impact of pumping was significantly stronger. Only 4 years after uncontrolled drilling activities had begun, the spring fell completely dry. Our models, which ignored the abstraction of groundwater, clearly indicated that the spring would have yielded considerable amounts of water until today. This was a clear proof that the decline of spring discharge cannot be the result of climate change.

Overall, we can conclude that a reduction of spring discharge due to climate change is uncertain for the near future but will most probably occur in the remote future. However, considering recent data, it is quite obvious that human impact, i.e. increased pumping from the aquifer, poses a much higher threat to spring water resources in the region of Faria spring. This calls for a better management of groundwater abstractions to meet future water needs which is especially true for the drought-prone Mediterranean region.

Acknowledgements

This study was supported by the GLOWA-Jordan River Project funded by the German Ministry of Education and Research (BMBF). We acknowledge the E-OBS dataset from the EU-FP6 Project ENSEMBLES (http://www.ensembles-eu.org) and the data providers in the ECA&D Project (http://eca.knmi.nl)". Gridded precipitation in the JR region was obtained from Lucas Menzel, University of Heidelberg, Germany.

References

Alpert, P., Krichak, S.O., Shafir, H., Haim, D., Osetinsky, I., 2008. Climatic trends to extremes employing regional modeling and statistical interpretation over the E. Mediterranean. Global Planet. Change 63, 163–170.

Andreo, B., Goldscheider, N., Vadillo, I., Vías, J.M., Neukum, C., Sinreich, M., Jiménez, P., Brechenmacher, J., Carrasco, F., Hötzl, H., 2006. Karst groundwater protection: first application of a Pan-European approach to vulnerability, hazard and risk mapping in the Sierra de Líbar (Southern Spain). Sci. Total Environ. 357 (1–3), 54–73. http://dx.doi.org/10.1016/j.scitotenv.2005.05.019.

Bergström, S., 1995. The HBV model. In: Singh, V.P. (Ed.), Computer Models of Watershed Hydrology. Water Resources Publications, Highlands Ranch, CO.

Beven, K.J., 1989. Changing ideas in hydrology – the case of physically-based models. J. Hydrol. 105 (1–2), 157–172. http://dx.doi.org/10.1016/0022-1694(89)90101-7.

Beven, K.J., Kirby, M.J., 1979. A physically based, variable contributing area model of basin hydrology. Hydrol. Sci. Bull. 24, 43–69.

Brooks, D., Trottier, J., 2010. Confronting water in an Israeli–Palestinian peace agreement. J. Hydrol. 382 (1–4), 103–114.

Brouyère, S., Carabin, G., Dassargues, A., 2003. Climate change impacts on groundwater resources: modelled deficits in a chalky aquifer, Geer basin, Belgium. Hydrogeol. J. 12 (2). http://dx.doi.org/10.1007/s10040-003-0293-1.

Butscher, C., Huggenberger, P., 2008. Intrinsic vulnerability assessment in karst areas: a numerical modeling approach. Water Resour. Res. 44 (W03408). http://dx.doi.org/10.1029/2007WR006277.

Chenoweth, J., Hadjinicolaou, P., Bruggeman, A., Lelieveld, J., Levin, Z., Lange, M.A., Xoplaki, E., Hadjikakou, M., 2011. Impact of climate change on the water resources of the Eastern Mediterranean and Middle East region: modeled 21st century changes and implications. Water Resour. Res. 47 (6). http://dx.doi.org/10.1029/2010wr010269.

Crosbie, R.S., Dawes, W.R., Charles, S.P., Mpelasoka, F.S., Aryal, S., Barron, O., Summerell, G.K., 2011. Differences in future recharge estimates due to GCMs, downscaling methods and hydrological models. Geophys. Res. Lett. 38 (11). http://dx.doi.org/10.1029/2011gl047657.

Déqué, M., Rowell, D.P., Lüthi, D., Giorgi, F., Christensen, J.H., Rockel, B., Jacob, D., Kjellström, E., de Castro, M., van den Hurk, B., 2007. An intercomparison of regional climate simulations for Europe: assessing uncertainties in model projections. Climatic Change. http://dx.doi.org/10.1007/s10584-006-9228-x.

Duan, Q.Y., Sorooshian, S., Gupta, H.V., 1992. Effective and efficient global optimization for conceptual rainfall–runoff models. Water Resour. Res. 28 (4), 1015–1031.

Dudhia, J., 1993. A nonhydrostatic version of the Penn State-NCAR mesoscale model: validation tests and simulation of an Atlantic cyclone and cold front. Mon. Weather Rev. 121, 1493–1513. http://dx.doi.org/10.1007/s10584-006-9228-x.

EXACT, 1998. Overview of Middle East Water Resources – Water Resources of Palestinian, Jordanian, and Israeli Interest. Compiled by the US Geological Survey for Executive Action Team Washington, p. 44. ISBN: 0-607-91785-7.

Fleury, P., Plagnes, V., Bakalowicz, M., 2007. Modelling of the functioning of karst aquifers with a reservoir model: application to Fontaine de Vaucluse (South of France). J. Hydrol. 345, 38–49.

Fleury, P., Ladouche, B., Conroux, Y., Jourde, H., Dörfliger, N., 2009. Modelling the hydrologic functions of a karst aquifer under active water management – the Lez spring. J. Hydrol. 365 (3–4), 235–243.

Garrido, A., Martínez-Santos, P., Llamas, M.R., 2006. Groundwater irrigation and its implications for water policy in semiarid countries: the Spanish experience. Hydrogeol. J. 14 (3), 340–349. http://dx.doi.org/10.1007/s10040-005-0006-.

Geyer, T., Birk, S., Licha, T., Liedl, R., Sauter, M., 2007. Multitracer test approach to characterize reactive transport in karst aquifers. Ground Water 45 (1), 36–45.
Geyer, T., Birk, S., Liedl, R., Sauter, M., 2008. Quantification of temporal distribution of recharge in karst systems from spring hydrographs. J. Hydrol. 348, 452–463.
Giorgi, F., Lionello, P., 2008. Climate change projections for the Mediterranean region. Global Planet. Change 63 (2–3), 90–104. http://dx.doi.org/10.1016/j.gloplacha.2007.09.005.
Goldscheider, N., Drew, D., 2007. In: Hydrogeologists, I.A.o. (Ed.), Methods in Karst Hydrogeology. Taylor & Francis Group, p. 264, ISBN: 978-0-415-42873-6.
Hao, Y., Yeh, T.-C.J., Gao, Z., Wang, Y., Zhao, Y., 2006. A gray system model for studying the response to climatic change: the Liulin karst springs, China. J. Hydrol. 328 (3–4), 668–676. http://dx.doi.org/10.1016/j.jhydrol.2006.01.022.
Hao, Y.H., Wang, Y.J., Zhu, Y., Lin, Y., Wen, J.C., Yeh, T.C.J., 2009. Response of karst springs to climate change and anthropogenic activities: the Niangziguan Springs, China. Prog. Phys. Geogr. 33 (5), 634–649. http://dx.doi.org/10.1177/0309133309346651.
Hargreaves, G.H., Samani, Z.A., 1985. Reference crop evapotranspiration from temperature. Appl. Eng. Agric. 1 (2), 96–99.
Hartmann, A., Kralik, M., Humer, F., Lange, J., Weiler, M., 2012. Identification of a karst system's intrinsic hydrodynamic parameters: upscaling from single springs to the whole aquifer. Environ. Earth Sci. 65 (8), 2377–2389. http://dx.doi.org/10.1007/s12665-011-1033-9.
Haylock, M., Hofstra, N., Tank, A.K., Klok, E., Jones, P., New, M., 2008. A European daily high-resolution gridded dataset of surface temperature and precipitation for 1950–2006. J. Geophys. Res. 113. http://dx.doi.org/10.1029/2008JD010201.
Heckl, A., 2011. Impact of Climate Change on the Water Availability in the Near East and the Upper Jordan River Catchment. PhD Thesis, Augsburg University, Augsburg, p. 194.
Jakeman, A.J., Hornberger, G.M., 1993. How much complexity is warranted in a rainfall–runoff model? Water Resour. Res. 29, 2637–2649.
Jukic, D., Denic-Jukic, V., 2009. Groundwater balance estimation in karst by using a conceptual rainfall–runoff model. J. Hydrol. 373 (3–4), 302–315.
Klemeš, V., 1986. Dilettantism in hydrology: transition or destiny. Water Resour. Res. 22 (9), 177S–188S.
Krichak, S.O., Breitgand, J., Samuels, R., Alpert, P., 2011. A double resolution transient rcm climate change simulation experiment for near coastal eastern zone of the Eastern Mediterranean region. Theor. Appl. Climatol. 103 (1–2), 167–195.
Lenderink, G., Buishand, A., van Deursen, W., 2007. Estimates of future discharges of the river Rhine using two scenario methodologies: direct versus delta approach. Hydrol. Earth Syst. Sci. 11 (3), 1145–1159. http://dx.doi.org/10.5194/hess-11-1145-2007.
Lewin, J., Woodward, J.C., 2009. Karst geomorphology and environmental change. In: Woodward, J.C. (Ed.), The Physical Geography of the Mediterranean. Oxford University Press, Oxford, pp. 287–318.
Loaiciga, H.A., Maidment, D.R., Valdes, J.B., 2000. Climate-change impacts in a regional karst aquifer, Texas, USA. J. Hydrol. 227 (1–4), 173–194. http://dx.doi.org/10.1016/s0022-1694(99)00179-1.
Maillet, E., 1905. Essais d'hydraulique souterraine et fluviale. In: Hermann, A., (Ed.), Mécanique et Physique du Globe, Paris.
Menzel, L., Koch, J., Onigkeit, J., Schaldach, R., 2009. Modelling the effects of land-use and land-cover change on water availability in the Jordan River region. Adv. Geosci. 21, 73–80. http://dx.doi.org/10.5194/adgeo-21-73-2009.
Nash, J.E., Sutcliffe, J.V., 1970. River flow forecasting through conceptual models. Part I: A discussion of principles. J. Hydrol. 10, 282–290.
Orlowsky, B., Seneviratne, S.I., 2012. Global changes in extreme events: regional and seasonal dimension. Clim. Change 110 (3–4), 669–696. http://dx.doi.org/10.1007/s10584-011-0122-9.
Pal, J.S., Small, E.E., Eltahir, E.A.B., 2000. Simulation of regional scale water and energy budgets: representation of subgrid cloud and precipitation processes within RegCM. J. Geophys. Res. 105, 29,579–29,594.
PWA, 2000. Summary of Palestinian Hydrologic Data 2000, volume 1: West Bank. In: El-Sharif, N., Kawash, F. (Eds.), Palestinian Water Authority. West Bank Water Data Bank Section, Ramallah.
Rimmer, A., Hartmann, A., 2012. Simplified conceptual structures and analytical solutions for groundwater discharge using reservoir equations. In: Nayak, D.P.C. (Ed.), Water Resources Management and Modeling. InTech, Kakinada, India, ISBN: 978-953-51-0246-5.
Rimmer, A., Salingar, Y., 2006. Modelling precipitation–streamflow processes in karst basin: the case of the Jordan River sources, Israel. J. Hydrol. 331, 524–542.
Samuels, R., Rimmer, A., Hartmann, A., Krichak, S., Alpert, P., 2010. Climate change impacts on jordan river flow: downscaling application from a regional climate model. J. Hydrometeorol. 11 (4), 860–879. http://dx.doi.org/10.1175/2010JHM1177.1.
Samuels, R., Smiatek, G., Krichak, S., Kunstmann, H., Alpert, P., 2011. Extreme value indicators in highly resolved climate change simulations for the Jordan River area. J. Geophys. Res. 116 (D24). http://dx.doi.org/10.1029/2011jd016322.
Sauter, M., Kovács, A., Geyer, T., Teutsch, G., 2006. Modellierung der hydraulik von karstgrundwasserleitern – eine übersicht. Grundwasser 3, 143–156.
Seiler, K.P., Gat, J.R., 2007. Groundwater Recharge from Run-off and Infiltration. Springer Verlag, Dordrecht.
Shadeed, S., Lange, J., 2010. Rainwater harvesting to alleviate water scarcity in dry conditions: a case study in Faria Catchment, Palestine. Water Sci. Eng. 3 (2), 132–143. http://dx.doi.org/10.3882/j.issn.1674-2370.2010.02.002.
Smiatek, G., Kunstmann, H., Heckl, A., 2011. High-resolution climate change simulations for the Jordan River area. J. Geophys. Res. 116 (D16). http://dx.doi.org/10.1029/2010jd015313.
Stoll, S., Hendricks Franssen, H.J., Butts, M., Kinzelbach, W., 2010. Analysis of the impact of climate change on groundwater related hydrological fluxes: a multi-model approach including different downscaling methods. Hydrol. Earth Syst. Sci. 15 (1), 21–23. http://dx.doi.org/10.5194/hess-15-21-2011.
Tritz, S., Guinot, V., Jourde, H., 2011. Modelling the behaviour of a karst system catchment using non-linear hysteretic conceptual model. J. Hydrol. 397 (3–4), 250–262. http://dx.doi.org/10.1016/j.jhydrol.2010.12.001.
van den Besselaar, E., Haylock, M., van der Schrier, G., Klein Tank, A.M.G., 2011. A European daily high-resolution observational gridded data set of sea level pressure. J. Geophys. Res. http://dx.doi.org/10.1029/2010JD015468.
Wagener, T., Boyle, D.P., Lees, M.J., Wheater, H.S., Gupta, H.V., Sorooshian, S., 2001. A framework for development and application of hydrological models. Hydrol. Earth Syst. Sci. 5 (1), 13–26.